land

Article

Assessment of the Ecological Condition of Informal Settlements Using the Settlement Surface Ecological Index

Naledzani Mudau [1,2,*] and Paidamwoyo Mhangara [1]

1 School of Geography, Archaeological & Environmental Studies, Faculty of Science, University of the Witwatersrand, Johannesburg 2000, South Africa; paida.mhangara@wits.ac.za
2 South African National Space Agency, Mark Shuttleworth Street, Innovation Hub Enterprise Building, Pretoria 0184, South Africa
* Correspondence: nmudau@sansa.org.za

Abstract: To manage urban ecological ecosystems adequately, understanding the urban areas' biophysical characteristics is required. This study developed a settlement surface ecological index (SSEI) using tree, soil, impervious surface and grass covers, land surface temperature (LST), and soil moisture derived from Satellite Pour L'Observation de la Terre (SPOT) 7 and Landsat 8 satellite images. The assessment of the SSEI was conducted over twelve sites of 300 m by 300 m. The selected sites contained formal and informal settlements of varying building densities. The SSEI values ranged from −0.3 to 0.54. Seven assessed areas are in the worst ecological condition with an SSEI below zero. Only three settlement types had an SSEI index value of 0.2 and above, and two of these areas were informal settlements. The formal low-density settlement with higher tree coverage displayed the highest index value of 0.54, slightly higher than the medium-density informal settlement. Overall, there is no significant difference in the SSEI values between the surface ecological condition of formal and informal settlements. The results achieved in this study can be used to understand urban ecology better and develop urban greening strategies at a city or settlement level.

Keywords: informal settlements; land surface temperature; urban ecology

check for updates

Citation: Mudau, N.; Mhangara, P. Assessment of the Ecological Condition of Informal Settlements Using the Settlement Surface Ecological Index. *Land* **2023**, *12*, 1622. https://doi.org/10.3390/land12081622

Academic Editor: Jianjun Zhang

Received: 18 June 2023
Revised: 10 August 2023
Accepted: 12 August 2023
Published: 17 August 2023

1. Introduction

The urban ecosystem provides services that directly impact human health and security, including runoff mitigation, urban cooling, and air purification [1]. The availability of vegetation in urban areas can help improve air quality and reduce flood severity [2]. In addition, improving green infrastructure in informal settlements can help enhance social and cultural interaction [3,4]. In addition, an increase in the impervious surface and low vegetation cover negatively affects the local microclimate and increases the formation of surface urban heat island (SUHI) [5]. Exposure to excessive heat in certain areas can cause physiological and socio-economic stress, amplify existing health issues, and increase premature death or disability [6]. Populations in informal settlements are likely to be affected the most by increased heat exposure as the dwelling structures in these areas lack cooling services [7]. Urbanization can also result in soil erosion or contamination, which may threaten human health [8].

Satellite images have been widely used to assess and detect land use features such as human settlement developments [9–12], informal settlements [13–15], and urban growth rates [16,17]. Vegetation cover and density of impervious surface are the two land cover classes that have been thoroughly investigated in an attempt to automatically detect informal settlements from satellite imagery [18–20]. Other studies have used satellite images to map and measure urban morphology [21,22].

Urban surfaces and their characteristics play an important role in achieving sustainable and resilient cities as they can influence the people's quality of life and the settlements' environmental conditions [23]. Several studies have assessed the environmental conditions of cities using a vegetation-impervious surface-soil (VIS) model [24] and medium spatial resolution images [25,26]. In addition to the VIS model, assessing other biophysical characteristics such as surface temperature, wetness, and air quality provides more variables to assess the surface ecological status of cities. The remote sensing ecological index (RSEI) is the first model that utilizes remotely sensed data to assess the status of the urban ecology of cities [27]. RSEI uses vegetation index, humidity, land surface temperature, and built-up and bareness index [27]. Researchers have explored the RSEI to evaluate the status of urban ecology across cities [28–30].

The methodologies commonly used for mapping the land cover biophysical characteristics include the thresholding radiometric values and the maximum-likelihood algorithm (MLA]. Due to the heterogeneity of land use features in urban areas, these methods suffer from spectral mixing issues. A hierarchical algorithm that uses textural features has proven to perform better than MLA [31]. Using object-based image analysis (OBIA) in mapping urban land cover using high-resolution imagery improves the results significantly compared to pixel-based classification and MLA [32].

The previous studies conducted on the assessment of ecological studies are limited to a city level, providing data required to develop a city-level intervention. Since informal settlements are illegal and may lack essential services such as sanitation, water, and waste removal [33], they pose several social and environmental challenges. Environmental challenges such as land degradation and pollution of natural resources have been associated with informal settlements [34]. This may be attributed to unmanaged land use activities and lack of access to basic services [33]. In addition, the effect of climate change and global change may be more severe in informal settlements than in formal settlements as they are located in undesirable locations such as flood-prone or high-slope areas [35]. With future urbanization expected to take place mostly in developing countries that are already struggling with informal settlement developments, understanding the vulnerability of informal settlements can help develop interventions to improve the wellbeing of people living in informal settlements.

The studies that used RSEI to assess the ecological conditions of the cities assess the broad land-use classes. Since human settlements are not the same, a detailed analysis of urban ecological conditions is required to improve understanding of urban environments and develop necessary solutions to build green infrastructure across a city. This study builds on RSEI and develops a settlement surface ecological index (SSEI) that uses the tree, grassland, impervious surface, soil, land surface temperature, and vegetation moisture to assess the ecological status of informal and formal settlements using biophysical parameters derived from high and medium spatial resolution imagery.

2. Study Area

The study area covers residential, commercial, and industrial areas in the eastern part of the City of Tshwane, Gauteng, South Africa, and lies between $-25°41'$ and $-25°46'$ latitude and $28°17'$ and $28°26'$ longitude. The study area contains low- and high-density residential areas on the eastern side of the metropolitan municipality and formal high-density and informal settlements in Mamelodi township, located about 30 km from the city's central business district; see Figure 1: Location of the study area and different human settlement types assessed in the study.

The main economic activities in the municipality are finance and manufacturing. About 16% of municipal households were informal settlements in 2016 [36]. Mamelodi is one of the townships experiencing increased development of informal settlements [37]. The municipality plans to upgrade informal settlements by providing essential services or top structures [38]. In addition, several initiatives are aimed at greening the cities to improve air quality and sociocultural interaction, especially in townships. The zoom-in pictures of selected areas are shown in Appendix A.

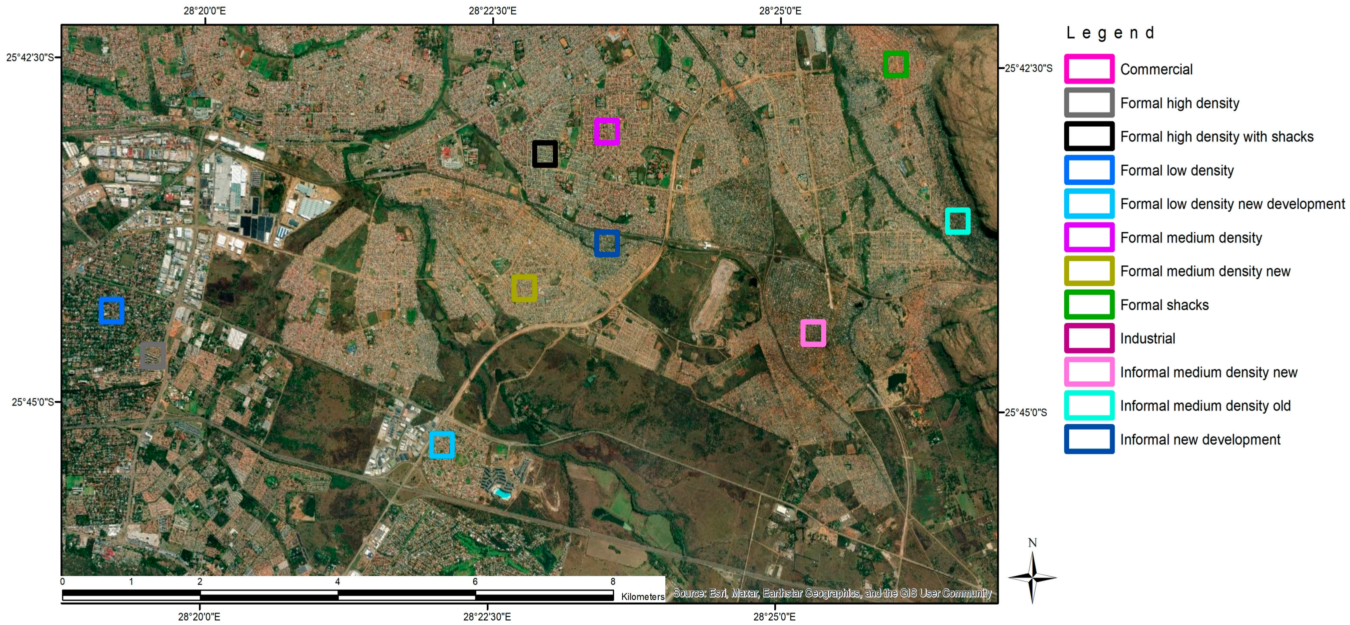

Figure 1. Location of the study area and different human settlement types assessed in the study.

The selection of the different human settlement types was performed through visual interpretation using the Google Earth platform. The maps of the selected settlement were generated using Esri base maps. The description of the selected settlements was guided by Census 2011 metadata [39] and the South African National Land Cover Classification standard, 19144-2:2014.

3. Data

We used Satellite Pour Observation de la Terre (SPOT) 7 images acquired on 8 November 2017 to classify urban land cover classes. The SPOT 7 sensor acquires images both in multispectral and panchromatic modes. The scene IDs of the images used are IMG_SPOT7_MS_201711070754099_ORT_SPOT7_20180925_0743431nq51eejut843_1_R3C2 and img_spot7_ms_201711070754099_ort_spot7_20180925_0743431nq51eejut843_1_r3c2. The spectral bands, wavelength, and spatial resolution of SPOT 7 are presented in Table 1.

Table 1. List of the spectral band, bandwidth, and spatial resolutions of SPOT 7 and Landsat 8 satellite images.

Spectral Band	Wavelength (μm)	Spatial Resolution (m)
	SPOT 7	
Panchromatic	0.45–0.75	1.5
Blue	0.45–0.52	6
Green	0.53–0.06	6
Red	0.62–0.69	6
Near-Infrared	0.76–0.89	6
	Landsat 8	
Panchromatic	0.50–0.68	15
Coastal Blue	0.43–0.45	30
Blue	0.45–0.67	30

Table 1. *Cont.*

Spectral Band	Wavelength (µm)	Spatial Resolution (m)
Green	0.53–0.59	30
Red	0.64–0.67	30
Near-Infrared	0.85–0.88	30
Short-wave Infrared1	1.57–1.65	30
Short-wave Infrared 2	2.11–2.29	30
Cirrus	1.36–1.38	30
Thermal Infrared 1	10.6–11.19	100
Thermal Infrared 2	11.50–12.51	100

A Landsat 8 image acquired on 08 November 2017, scene ID LC81700782017312LGN00, was used to derive land surface temperature and vegetation moisture information.

4. Methodology

4.1. Classification of Urban Land-Use Classes

The classification of impervious surface tree, grass, and soil cover and features from the SPOT 7 satellite image was performed using the object-based image analysis (OBIA) technique in Trimble eCognition Software. The OBIA technique has been widely used to detect urban land cover and land use classes from high spatial resolution satellite imagery [18,40]. This technique has generated more accurate results than pixel-based urban land use classification [32]. The first fundamental step of OBIA is image segmentation. This process partitions an image into image objects that represent desired land use or land cover features with similar spectral and spatial properties [41]. The quality of results achieved using OBIA techniques depends on the image objects created during image segmentation [41].

The multiresolution segmentation method was used to partition the image into image objects. This bottom-up, region-merging technique partitions an image into objects based on the user-defined homogeneity criteria, i.e., scale, compactness, and shape [42]. Two segmentation levels were created using 400 and 25 scale parameters using the multispectral bands. Segmentation parameters were selected using the trial-and-error method by visually inspecting segmentation results. The scale parameter 400 generated Level 1 image objects representing non-built-up and built-up land cover and land use classes. In contrast, the scale parameter 25 generated Level 2 image objects representing urban land use objects. The compactness and shape parameters of 0.5 and 0.1 were selected for both segmentation levels. The scale, compactness, and shape parameters were selected using trial and error by visually inspecting the results and adjusting the segmentation parameters [43,44].

The OBIA rule-based classification technique was used to classify level 1 image objects into built-up and non-built-up classes. A ruleset that uses radiometric values, vegetation indices and textural features was developed to classify built-up and non-built-up classes. Classifying built-up and non-built-up areas using the gray-level co-occurrence matrix (GLCM) dissimilarity texture [45]. The GLCM dissimilarity texture measures the distance between pairs of pixels within an image object [45]. Due to the heterogeneity of land use features in urban areas, the dissimilarity values are expected to be higher dissimilarity texture values than in non-built-up areas [12]. Most image objects in urban areas are also expected to have higher brightness values than non-built-up areas [46]. A rule set that uses GLCM dissimilarity and brightness values is expected to separate built-up and non-built-up areas.

Level 2 image objects were classified into trees, grass, impervious surface, and soil using the soil-adjusted vegetation index (SAVI) [47], GLCM dissimilarity texture [45], Pantex [48], and iron oxide index [49].

The SAVI is a vegetation index that minimizes the impact of soil properties in vegetated areas [47]. The SAVI has been widely used to map vegetation from other land cover classes, such as impervious surfaces, soil, and water [50,51]. The impervious surfaces, including roads and building structures, are expected to have lower SAVI values than soil and vegetation classes [52,53]. SAVI was used to classify trees from grass features.

Pantex is a texture-derived built-up presence that uses GLCM for different directions and displacements and has proven to improve the classification of human settlement land use types compared to other built-up indices [48]. Building structures are expected to have higher Pantex values than other land-use classes [48].

The GLCM dissimilarity texture was used to distinguish open areas from building structures. The iron oxide or iron index measures the amount of iron on the surface using the red and blue bands [49]. This index was used to distinguish grass from soil classes. SAVI was used to classify trees from grass features.

4.2. Mapping of Land Surface Temperature

LST was derived using band 10 of the Landsat 8 satellite. The LST was calculated using the following formula:

$$LST = \frac{BT}{1 + (\lambda \mathrm{BT}/\rho)\ln\varepsilon} \tag{1}$$

where BT is brightness temperature, λ is the length of emitted wavelength, ρ is a constant obtained using the formula $h * \frac{c}{\sigma}$, where h is Plank's constant, c is the velocity of light, σ is the Boltzmann constant, and Ɛ is land surface emissivity.

4.3. Mapping of Vegetation Moisture

The assessment of vegetation moisture in the study area was performed by analyzing the normalized difference moisture index (NDMI), which measures vegetation water content. The NDMI was derived using the following formula:

$$NDMI = \frac{(NIR - SWIR1)}{(NIR + SWIR1)} \tag{2}$$

4.4. The Assessment of Settlement Surface Ecological Index

The SSEI is a function of the urban land cover classes, LST, and vegetation moisture, and it was calculated using the following formula:

$$\text{SSEI} = (\text{Tree cover} + \text{Grass cover} + \text{vegetation moistures}) - (\text{Impervious surface} + \text{LST}) \tag{3}$$

The assessment of SSEI index was performed over 300 m × 300 m of the selected urban land-use classes. The assessed biophysical characteristics were standardized to the 0–1 range. The index is defined as the difference between characteristics that improve urban ecology and those that negatively alter the urban ecosystem. The values of SSEI range from 0 to 1. Values closer to one represent a better settlement ecological condition, and values closer to zero represent the worst.

4.5. Quality Assurance

Quality assurance of mapped VIS classes was performed by assessing the classification results with the manually selected image objects representing the mapped classes. A total of 588 impervious surfaces, 71 trees, 42 grasses, and 99 soil samples were created through visual image interpretation using a random sampling method. The accuracy assessment used Trimble eCognition 9.0 software (41). We assessed overall, producer and user accuracies. These producer and user accuracy measurements assess the errors of omission and commission of selected samples on the classified image.

5. Results

5.1. Image Segmentation

Multiresolution image segmentation process with scale parameter, compactness and shape values of 400, 0.1, and 0.5, respectively, was able to generate built-up and non-built-up image objects; see Figure 2. The segmentation results show that non-built-up areas adjacent to built-up areas were accurately separated from built-up areas. The segmentation parameters also created image objects that represent different human settlement types. Some of the open spaces within settlements were separated from the residential area. There were, however, a few cases where open spaces objects were merged within residential areas image objects. The image objects in industrial and primarily commercial areas contained individual building structures since the building structures have clear contrast from the surrounding areas.

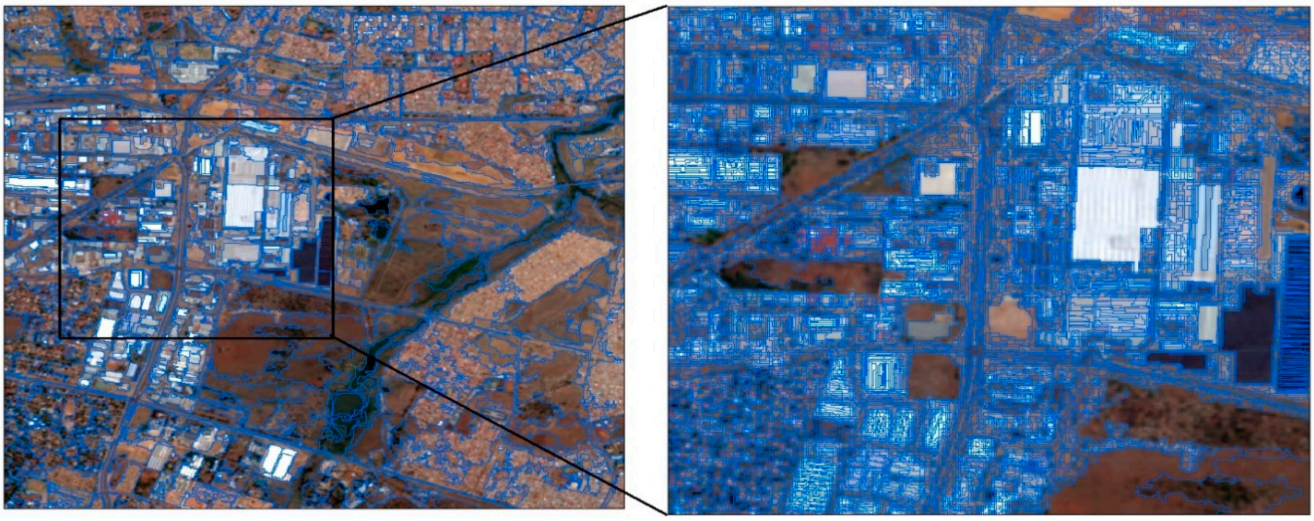

(**a**) (**b**)

Figure 2. Level 1 multiresolution segmentation results over SPOT 7 images (**a**) and Level 2 multiresolution segmentation results over SPOT 7 images (**b**).

The Level 2 multiresolution segmentation separated impervious surface, soil, and vegetation image objects. However, impervious surfaces, such as roads and building structures in industrial areas and in low-density settlements, experienced oversegmentation. Oversegmentation in low-density formal settlements may be attributed to the different orientations of the building structures.

Undersegmentation was observed in informal settlements where more than one building structure was merged into one image object.

5.2. Image Classification

The OBIA ruleset-based classification method that uses GLCM dissimilarity texture successfully classified built-up areas from non-built-up land cover classes, Figure 3 see Table 2. The major roads were successfully classified as built-up areas. Some areas with bare soil without building structures were classified as built-up areas. Image objects formed in such areas had apparent contrast differences from the surrounding non-built-up areas. Some open-space image objects with small human settlement segments were classified as non-built-up areas. Non-built-up areas are primarily found in the bottom left of the study area.

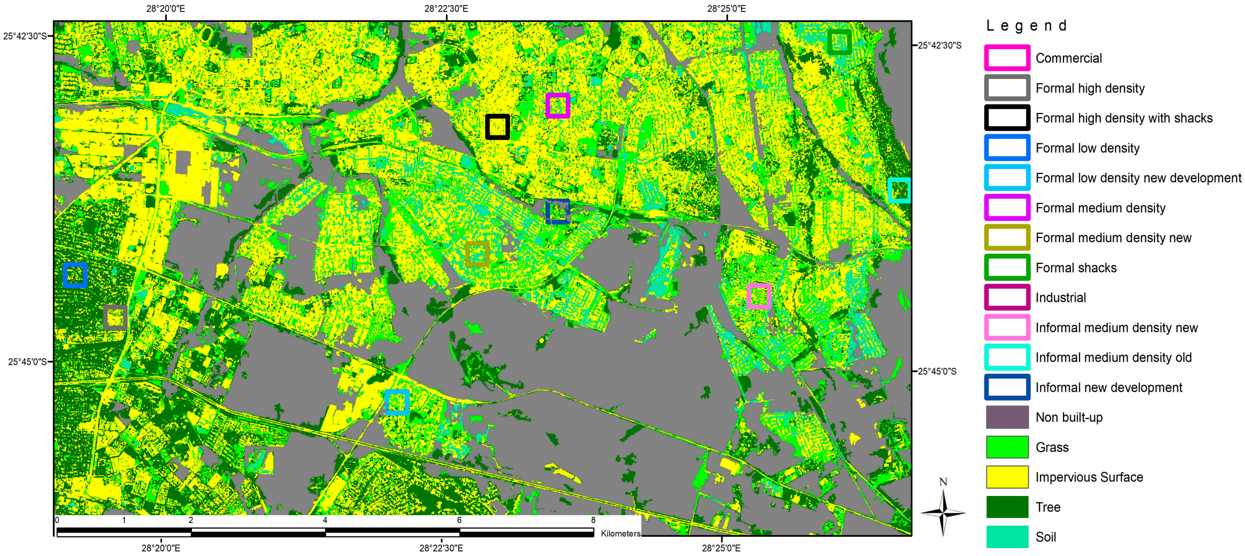

Figure 3. Classification results and the location of assessed settlements.

Table 2. Producer and user accuracies achieved during the classification of impervious surface, soil, grass, and tree cover.

Class	User Accuracy %	Producer Accuracy %
Impervious surface	97.9	94.4
Soil	87.2	82.8
Trees	89.7	98.6
Grass	66.6	63.6

The use of Pantex and dissimilarity texture was able to distinguish building structures from vegetation and soil because building structures in the study areas contain a clear contrast from the surrounding land use classes. The use of SAVI was able to separate trees from the grass class. The separation of bare soil and vegetated areas was successfully achieved using the iron index. The results show that the built-up areas on the bottom left of the study area contained higher tree coverage than the other built-up areas. In contrast, the rest of the built-up areas in the middle and top of the study area contain a higher percentage of impervious surface; see Figure 3. The soil class can be seen mainly from the center to the left and top right corner of the study area.

An overall accuracy of 91.1% was achieved in classifying trees, grass, impervious surface, and soil cover; see Table 2. The soil class achieved producer and user accuracies of less than 90% compared to the other classes. The error of omission in this class was found in the formal and informal settlements where gravel road segments were merged and classified as an impervious surface class or vegetation class.

The grass class achieved poor accuracy compared to other classes. Some of the grass objects were misclassified as trees. Some of the grass image objects were classified as trees. Some of the grass segments were misclassified as open spaces. Some of the building structures in informal settlements were not classified as impervious surfaces but misclassified as soil. That may be attributed to the fact that some of the dwelling structures in informal settlements are small structures and were merged with the soil image objects.

5.3. Assessment of Biophysical Characteristics

The spatial distribution of the assessed human settlement types over LST and vegetation moisture is shown in Figures 4 and 5.

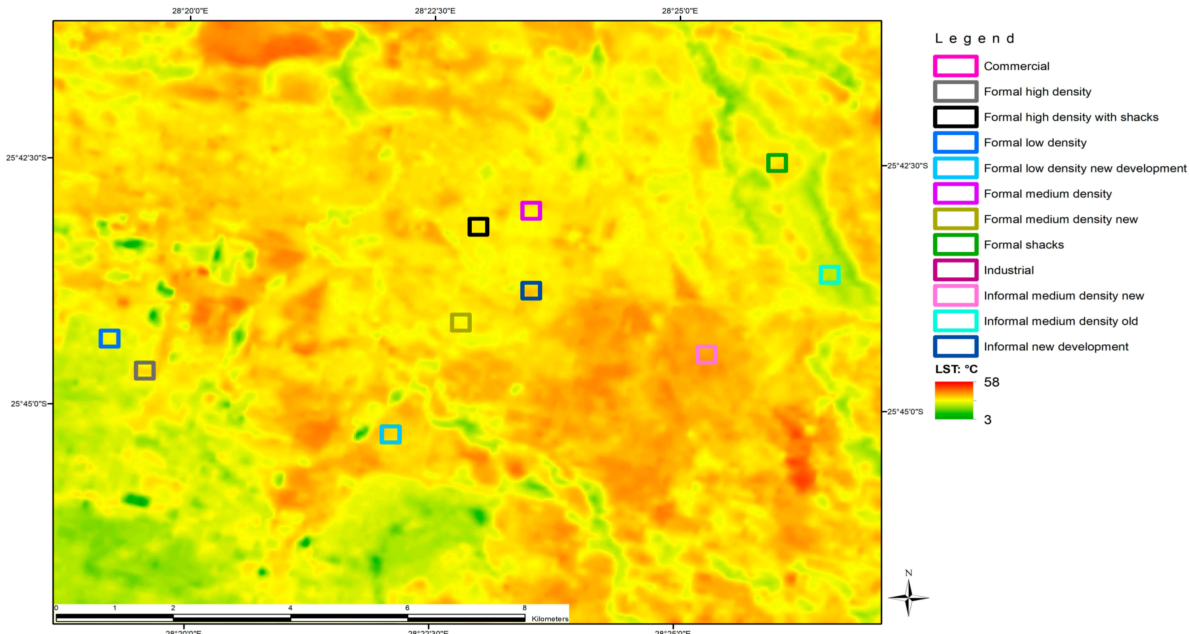

Figure 4. Spatial distribution of the different settlement types over the LST layer.

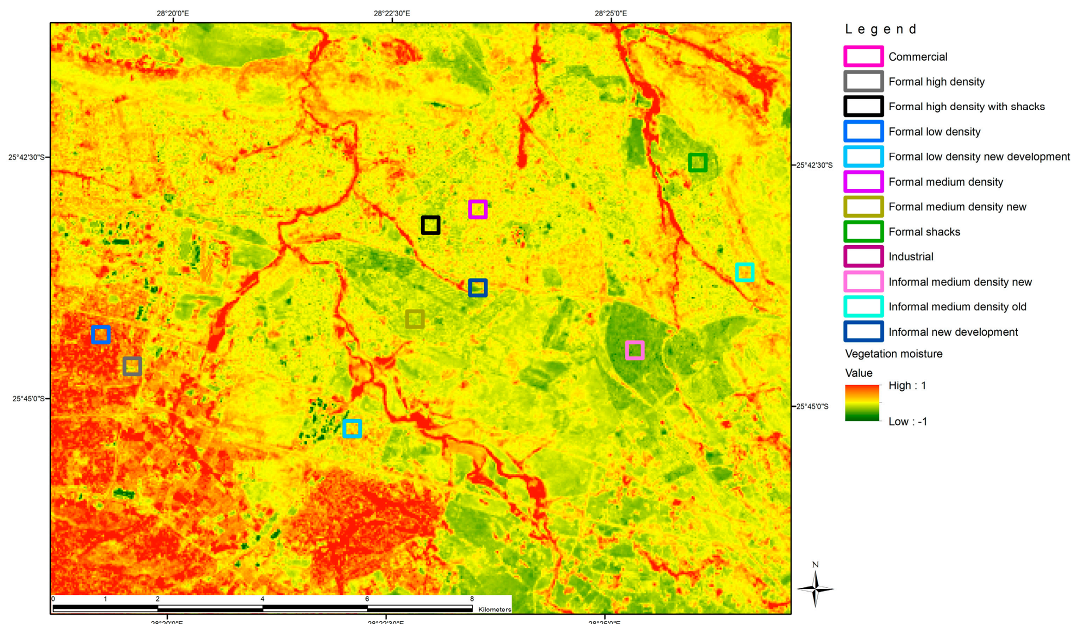

Figure 5. Spatial distribution of assessed settlement types over vegetation moisture layer.

The medium-density informal settlement experienced the highest LST of over 40 °C, and the old medium-density informal settlement experienced the lowest LST of 34 °C compared to other formal and informal settlement types; see Table 3. The lower LST in such an area may be attributed to the settlement located next to the mountain (53). The formal settlements experienced LST of 36–39 °C on the assessment day. The low-density formal settlement with high tree cover experienced the lowest LST, while the formal low-density new development experienced the highest LST. The LST in industrial areas was 1 °C higher than in commercial areas.

Table 3. Proportions and values of biophysical characteristics assessed during the study.

Settlement Type	LST _Mean	Soil %	Vegetation Moisture	Impervious Surface %	Tree %	Grass %
Commercial	36.90	0	0.00	77	19	3
Industrial	38.67	0	−0.02	90	4	6
Formal high density with shacks	38.31	1	−0.07	91	2	5
Formal medium density	37.88	16	−0.05	66	6	11
Formal shacks	38.70	48	−0.09	43	1	7
Old informal medium density	34.41	0	−0.02	31	63	6
Informal medium-density new development	42.67	3	−0.14	47	8	42
Formal low density	36.05	1	0.07	24	69	5
Formal low-density new development	39.16	3	−0.03	53	8	37
Formal medium-density new development	37.76	46	−0.08	49	0	4
Formal high density (clusters)	37.81	3	0.00	65	23	8
Informal new development	39.77	3	−0.06	17	47	33

The vegetation moisture was very low in all the settlement types, with values lower than 0.1; see Figure 5, Table 3. The settlements with the highest tree cover experienced the highest vegetation moisture of 0.07 compared to other settlement types.

The results show that the informal settlement class comprised less than 50% of the impervious surface, with new medium-density informal settlements containing the highest impervious surface cover of 49%. In comparison, the new informal settlements development contained the least impervious cover of 17%. The tree cover in informal settlements varied from 8% to 63%, with old informal settlements having the highest tree cover while the new medium-density informal settlement contained only 8% of tree cover. The soil cover in the informal settlements was extremely low, with a maximum cover of only 3%. The grass cover varied from 6% to 42%, with medium-density informal settlements having the highest grass cover compared to other informal settlement types.

Table 4 shows the normalized values of the assessed parameters. The normalized values were used to calculate the SSEI.

The low-density formal settlements had the highest composition of tree cover, 69%, compared to other settlement types. In contrast, medium formal density with backyard shacks and formal settlements with shacks had the lowest composition of trees. The soil cover was low in formal areas except in new formal density and formal settlements, with shacks with 46% and 48% cover. The impervious surface cover in formal settlements ranged between 24 and 91%. The low-density formal with a high cover of trees had the least impervious surface cover. The formal medium density with shacks had the highest impervious surface cover. Industrial areas had the second highest impervious surface cover of 90%, while the commercial area had the most impervious surface cover of 77%. Industrial and commercial areas had zero soil cover, with 10% and 22% vegetation, respectively.

5.4. Assessment of Settlement Surface Ecological Index (SSEI)

The status of urban surface ecology is good in low-density formal settlements compared to other settlement types; see Figure 6. The assessment of SSEI in informal settlements in the study areas varies according to the composition of the biophysical characteristics. The old medium-density informal settlement with a high cover of trees is in a better condition than the new medium-density informal settlement with a very low coverage of trees.

Table 4. Normalized values of the classification results.

Settlement Type	LST	Vegetation Moisture	Soil	Impervious Surface	Tree	Grass
Commercial	0.30	0.00	0.66	0.81	0.28	0.28
Industrial	0.52	0.00	0.59	0.99	0.06	0.06
Formal high density with shacks	0.47	0.00	0.30	1.00	0.03	0.03
Formal medium density	0.42	0.33	0.42	0.66	0.09	0.09
Formal shacks	0.52	1.00	0.20	0.35	0.01	0.01
Old informal medium density	0.00	0.00	0.59	0.19	0.91	0.91
Informal medium-density new development	1.00	0.06	0.00	0.41	0.12	0.12
Formal low density	0.20	0.02	1.00	0.09	1.00	1.00
Formal low-density new development	0.58	0.06	0.54	0.49	0.00	0.12
Formal medium-density new development	0.41	0.96	0.25	0.43	0.00	0.00
Formal high density (clusters)	0.41	0.06	0.67	0.65	0.33	0.33
Informal new development	0.65	0.06	0.37	0.00	0.68	0.68

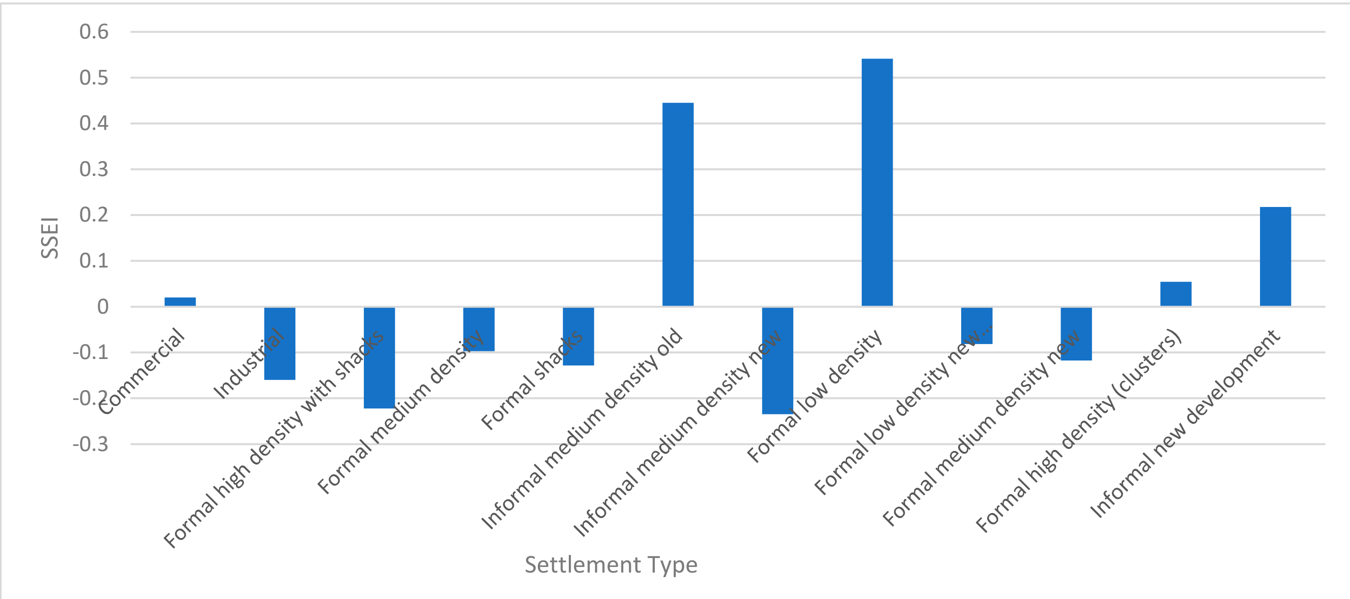

Figure 6. SSEI values of different settlement types.

Commercial area and formal medium-density clusters have the lowest positive SSEI values. All other settlement types have negative SSEI values, with the formal settlement with backyard shacks and new informal settlements having the worst ecological condition. Grass cover and soil cover have an insignificant negative correlation with the SSEI. Since moisture cover is positively correlated with tree cover, the results show that increasing the coverage of trees can improve the ecological conditions of the settlements, reduce surface temperature, reduce soil erosion, and reduce the impact of flooding.

The results show a need to improve the ecological conditions of medium-density informal and formal settlements. The SSEI can also be used during the planning of the interventions, i.e., tree planting strategies in areas with high cover of impervious surfaces may be different from those with low impervious surface cover.

6. Discussions

The condition of surface ecology is influenced by the physical, chemical, and biological characteristics of the area of interest and is affected by natural processes and land use activities. Several studies have assessed the ecological conditions of cities using VIS and RSEI extracted from medium spatial resolution images. The studies show that impervious surface cover affects the quality of the condition of surface ecology, with higher cover resulting in unhealthy surface ecological conditions [28,30]. These studies generated information that can support initiatives to manage and improve urban ecosystems at the city level. This study demonstrated that using biophysical parameters derived from high and medium spatial resolution images provides detailed information on the surface ecological conditions of different settlement types. The study shows that the surface ecological condition varies from one informal settlement to another. The results show that informal settlements with lower impervious surface and high tree cover have better ecological conditions than those with lower vegetation cover. The same trend was seen in formal settlements. This is well aligned with the previous studies that assessed ecological conditions using RSEI using medium spatial resolution conditions [29,30]. The results show that some of the formal settlements have unhealthy environmental conditions than some of the informal settlements. Such areas have higher impervious surface cover and lower tree cover. The assessment of the results shows that settlements with higher tree cover have better ecological conditions than those with higher grass cover. Informal settlements with higher grass cover and higher impervious surface were at an unhealthy surface ecological state compared to other assessed informal settlements. Further investigation on the impact of classifying grass from trees on SSEI needs to be conducted. The assessment of the index at different informal settlement types has the potential to provide valuable information that can be incorporated during the planning of upgrade projects. High spatial resolution imagery and information on the location of informal settlements are not always available and may be a limitation in assessing this index in certain countries or cities.

7. Conclusions

The study assessed the surface ecological conditions of informal settlements. The analysis of impervious surface, tree and grass cover, LST, and vegetation moisture provides valuable information on the environmental vulnerability of informal settlements and other settlement types. The results achieved in this study can be used to develop green strategies suitable for the different informal settlements to improve wellbeing. The results can also be used to develop disaster management strategies to reduce the impact of disasters on informal settlements. In addition, the information provided in this study can be used as input during the planning of informal settlement upgrade projects to ensure that the planning of services takes into account the need to reduce the environmental vulnerability of the settlements. As urbanization and the effects of climate change continue to be challenges for many city authorities, addressing the environmental challenges of informal and formal settlements is key to achieving sustainable development. The developed index contributes to ongoing research to build resilient settlements and offers practical measurements that can be used as the foundation for further work to understand the resilience of the cities.

Author Contributions: Conceptualization, N.M. and P.M.; methodology, N.M.; validation, N.M.; formal analysis, N.M.; investigation, N.M.; writing—original draft preparation, N.M.; writing—review and editing, N.M. and P.M. visualization, N.M.; supervision, P.M. All authors have read and agreed to the published version of the manuscript.

Funding: This research received no external funding.

Data Availability Statement: The data produced in this research may be made available upon request.

Conflicts of Interest: The authors declare no conflict of interest.

Appendix A

Settlement Type	Description	Picture
Old, informal medium density	Medium-density informal settlements with trees	
Informal medium density, new	Less than five-year-old informal settlement with medium building density	

Settlement Type	Description	Picture
Informal settlement density, new development	New, informal settlement developments, less than a year old	
Formal low density	Old suburb with a low building density of single- or double-story houses and big yards	

Settlement Type	Description	Picture
Formal low-density, new development	New development of formal low building density	
Formal medium density (cluster)	A formal medium building density where dwellings have private grounds within a common ground of other dwellings, located in a suburb	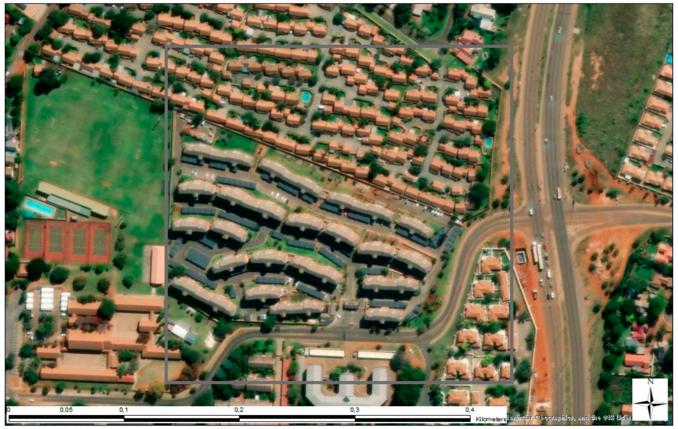

Settlement Type	Description	Picture
Formal medium density with backyard shacks	Formal townships with medium building density, located beyond the city limits, with backyard shacks	
Formal shacks	Serviced informal settlement, located in a township. Majority of the structures are shacks	

Settlement Type	Description	Picture
Formal medium density	Formal townships with medium building density located beyond the city limits	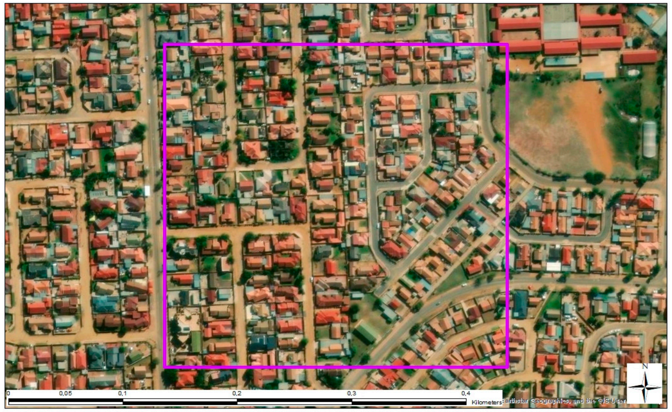
Formal medium density, new	Formal medium building density, less than five years old	

Settlement Type	**Description**	**Picture**
Commercial	A non-residential built-up surface area used to conduct commerce, and other areas. The selected area is located outside the central business district (CBD)	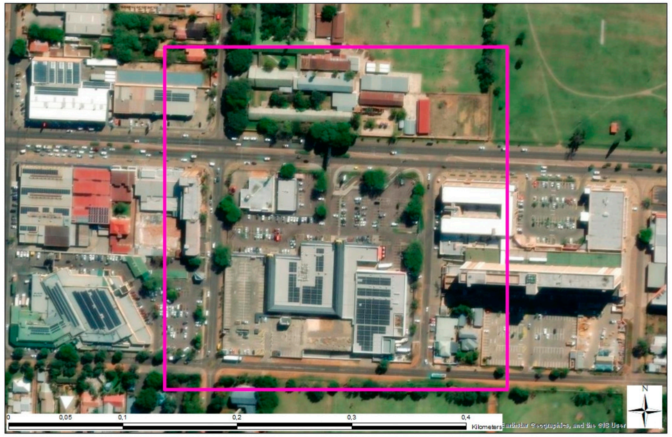
Industrial	A non-residential built-up surface area used for manufacturing or processing of products	

References

1. Bolund, P.; Hunhammar, S. Ecosystem services in urban areas. *Ecol. Econ.* **1999**, *29*, 293–301. [CrossRef]
2. Gallagher, J.; Baldauf, R.; Fuller, C.H.; Kumar, P.; Gill, L.W.; McNabola, A. Passive Methods for Improving Air Quality in the Built Environment: A Review of Porous and Solid Barriers. *Atmos. Environ.* **2015**, *120*, 61–70. Available online: https://www.sciencedirect.com/science/article/pii/S1352231015303204 (accessed on 11 August 2023). [CrossRef]
3. Adegun, O.B. Green Infrastructure Can Improve the Lives of Slum Dwellers in African Cities. *Front. Sustain. Cities* **2021**, *3*, 621051. [CrossRef]
4. Haase, D.; Kabisch, S.; Haase, A.; Andersson, E.; Banzhaf, E.; Baró, F.; Brenck, M.; Fischer, L.K.; Frantzeskaki, N.; Kabisch, N.; et al. Greening cities–To be socially inclusive? About the alleged paradox of society and ecology in cities. *Habitat Int.* **2017**, *64*, 41–48. Available online: https://www.sciencedirect.com/science/article/pii/S0197397516309390 (accessed on 11 August 2023). [CrossRef]
5. Morabito, M.; Crisci, A.; Guerri, G.; Messeri, A.; Congedo, L.; Munafò, M. Surface urban heat islands in Italian metropolitan cities: Tree cover and impervious surface influences. *Sci. Total Environ.* **2021**, *751*, 142334. Available online: https://www.sciencedirect.com/science/article/pii/S0048969720358630 (accessed on 11 August 2023). [CrossRef]
6. Anderson, B.; Bell, M. Weather-related mortality: How heat, cold, and heat waves affect mortality in the United States. *Epidemiology* **2009**, *20*, 205. [CrossRef]
7. Ramsay, E.E.; Fleming, G.M.; Faber, P.A.; Barker, S.F.; Sweeney, R.; Taruc, R.R.; Chown, S.L.; Duffy, G.A. Chronic heat stress in tropical urban informal settlements. *iScience* **2021**, *24*, 103248. Available online: https://www.sciencedirect.com/science/article/pii/S2589004221012177 (accessed on 11 August 2023). [CrossRef]
8. Wang, L.Y.; Xiao, Y.; Rao, E.M.; Jiang, L.; Xiao, Y.; Ouyang, Z.Y. An Assessment of the Impact of Urbanization on Soil Erosion in Inner Mongolia. *Int. J. Environ. Res. Public Health* **2018**, *15*, 550. Available online: https://www.mdpi.com/1660-4601/15/3/550 (accessed on 11 August 2023). [CrossRef]
9. Kemper, T.; Mudau, N.; Mangara, P.; Pesaresi, M. Towards an automated monitoring of human settlements in South Africa using high resolution SPOT satellite imagery. In *International Archives of the Photogrammetry, Remote Sensing and Spatial Information Sciences—ISPRS Archives*; International Society for Photogrammetry and Remote Sensing: Bethesda, MD, USA, 2015; pp. 1389–1394.
10. Pesaresi, M.; Politis, P. *GHS-BUILT-S R2022A—GHS Built-Up Surface Grid, Derived from Sentinel2 Composite and Landsat, Multitemporal (1975–2030)*; European Commission, Joint Research Centre (JRC): Brussels, Belgium, 2022.
11. Marconcini, M.; Metz-Marconcini, A.; Üreyen, S.; Palacios-Lopez, D.; Hanke, W.; Bachofer, F.; Zeidler, J.; Esch, T.; Gorelick, N.; Kakarla, A.; et al. Outlining where humans live, the World Settlement Footprint 2015. *Sci. Data* **2020**, *7*, 1–14. [CrossRef]
12. Mudau, N.; Mapurisa, W.; Tsoeleng, T.; Mashalane, M. Towards development of a national human settlement layer using high resolution imagery: A contribution to SDG reporting. *S. Afr. J. Geomat.* **2022**, *9*, 1–12. [CrossRef]
13. Gram-Hansen, B.J.; Helber, P.; Varatharajan, I.; Azam, F.; Coca-Castro, A.; Kopackova, V.; Bilinski, P. Mapping informal settlements in developing countries using machine learning and low resolution multi-spectral data. In Proceedings of the 2019 AAAI/ACM Conference on AI, Ethics, and Society, Honolulu, HI, USA, 27–28 January 2019; pp. 361–368.
14. Luo, E.; Kuffer, M.; Wang, J. Urban poverty maps–From characterising deprivation using geo-spatial data to capturing deprivation from space. *Sustain. Cities Soc.* **2022**, *84*, 104033. Available online: https://www.sciencedirect.com/science/article/pii/S2210670722003535 (accessed on 11 August 2023). [CrossRef]
15. Owusu, M.; Kuffer, M.; Belgiu, M.; Grippa, T.; Lennert, M.; Georganos, S.; Vanhuysse, S. Towards user-driven earth observation-based slum mapping. *Comput. Environ. Urban Syst.* **2021**, *89*, 101681. Available online: https://www.sciencedirect.com/science/article/pii/S0198971521000880 (accessed on 11 August 2023). [CrossRef]
16. Yadav, V.; Ghosh, S.K. Assessment and prediction of urban growth for a mega-city using CA-Markov model. *Geocarto Int.* **2021**, *36*, 1960–1992. [CrossRef]
17. Borana, S.L.; Vaishnav, A.; Yadav, S.K.; Parihar, S.K. Urban Growth Assessment Using Remote Sensing, GIS and Shannon's Entropy Model: A Case Study of Bhilwara City, Rajasthan. In Proceedings of the 2020 3rd International Conference on Emerging Technologies in Computer Engineering: Machine Learning and Internet of Things (ICETCE), Jaipur, India, 7–8 February 2020; pp. 1–6.
18. Mudau, N.; Mhangara, P. Investigation of informal settlement indicators in a densely populated area using very high spatial resolution satellite imagery. *Sustainability* **2021**, *13*, 4735. [CrossRef]
19. Fallatah, A.; Jones, S.; Mitchell, D.; Kohli, D. Mapping informal settlement indicators using object-oriented analysis in the Middle East. *Int. J. Digit Earth* **2019**, *12*, 802–824. [CrossRef]
20. Hofmann, P.; Strobl, J.; Blaschke, T.; Kux, H. Detecting informal settlements from QuickBird data in Rio de Janeiro using an object based approach. In *Object-Based Image Analysis*; Springer: Berlin/Heidelberg, Germany, 2008; pp. 531–553.
21. Chen, W.; Wu, A.N.; Biljecki, F. Classification of Urban Morphology with Deep Learning: Application on Urban Vitality. *Comput. Environ. Urban Syst.* **2021**, *90*, 101706. [CrossRef]
22. Wang, J.; Fleischmann, M.; Venerandi, A.; Romice, O.; Kuffer, M.; Porta, S. EO + Morphometrics: Understanding cities through urban morphology at large scale. *Landsc Urban Plan.* **2023**, *233*, 104691. [CrossRef]
23. Croce, S.; Vettorato, D. Urban surface uses for climate resilient and sustainable cities: A catalogue of solutions. *Sustain. Cities Soc.* **2021**, *75*, 103313. [CrossRef]

24. Ridd, M.K. Exploring a V-I-S (vegetation-impervious surface-soil) model for urban ecosystem analysis through remote sensing: Comparative anatomy for cities. *Int. J. Remote Sens.* **1995**, *16*, 2165–2185. [CrossRef]
25. Phinn, S.; Stanford, M.; Scarth, P.; Murray, A.T.; Shyy, P.T. Monitoring the composition of urban environments based on the vegetation-impervious surface-soil (VIS) model by subpixel analysis techniques. *Int. J. Remote Sens.* **2002**, *23*, 4131–4153. [CrossRef]
26. Aina, Y.A.; Adam, E.; Ahmed, F.; Wafer, A.; Alshuwaikhat, H.M. Using multisource data and the V-I-S model in assessing the urban expansion of Riyadh city, Saudi Arabia. *Eur. J. Remote Sens.* **2019**, *52*, 557–571. [CrossRef]
27. Hu, X.; Xu, H. A new remote sensing index for assessing the spatial heterogeneity in urban ecological quality: A case from Fuzhou City, China. *Ecol. Indic.* **2018**, *89*, 11–21. Available online: https://www.sciencedirect.com/science/article/pii/S1470160$\times$18300827 (accessed on 11 August 2023). [CrossRef]
28. Yue, H.; Liu, Y.; Li, Y.; Lu, Y. Eco-Environmental Quality Assessment in China's 35 Major Cities Based On Remote Sensing Ecological Index. *IEEE Access* **2019**, *7*, 51295–51311. [CrossRef]
29. Firozjaei, M.K.; Fathololoumi, S.; Weng, Q.; Kiavarz, M.; Alavipanah, S.K. Remotely sensed urban surface ecological index (RSUSEI): An analytical framework for assessing the surface ecological status in urban environments. *Remote Sens.* **2020**, *12*, 2029. [CrossRef]
30. Li, J.; Gong, J.; Guldmann, J.M.; Yang, J. Assessment of urban ecological quality and spatial heterogeneity based on remote sensing: A case study of the rapid urbanization of wuhan city. *Remote Sens.* **2021**, *13*, 4440. [CrossRef]
31. Setiawan, H.; Mathieu, R.; Thompson-Fawcett, M. Assessing the applicability of the V–I–S model to map urban land use in the developing world: Case study of Yogyakarta, Indonesia. *Comput. Environ. Urban Syst.* **2006**, *30*, 503–522. Available online: https://www.sciencedirect.com/science/article/pii/S0198971505000360 (accessed on 11 August 2023). [CrossRef]
32. Myint, S.W.; Gober, P.; Brazel, A.; Grossman-Clarke, S.; Weng, Q. Per-pixel vs. object-based classification of urban land cover extraction using high spatial resolution imagery. *Remote Sens. Environ.* **2011**, *115*, 1145–1161. [CrossRef]
33. UN-Habitat. The challenge of slums: Global report on human settlements 2003. *Manag. Environ. Qual. Int. J.* **2004**, *15*, 337–338. [CrossRef]
34. Devi, P.P.; Lowry, J.H.; Weber, E. Global environmental impact of informal settlements and perceptions of local environmental threats: An empirical case study in Suva, Fiji. *Habitat Int.* **2017**, *69*, 58–67. Available online: https://www.sciencedirect.com/science/article/pii/S0197397516310293 (accessed on 11 August 2023). [CrossRef]
35. Ramin, B. Slums, climate change and human health in sub-Saharan Africa. *Bull. World Health Organ.* **2009**, *87*, 886. Available online: https://europepmc.org/articles/PMC2789375 (accessed on 11 August 2023). [CrossRef]
36. Cooperative Governance and Traditional Affairs. 2020. Available online: https://www.cogta.gov.za/index.php/page/36/?option=com_docman&task=cat_view&gid=111&limit=5&limitstart=5&order=name&dir=ASC (accessed on 11 August 2023).
37. Mudau, N.; Mhangara, P. Towards understanding informal settlement growth patterns: Contribution to SDG reporting and spatial planning. *Remote Sens Appl.* **2022**, *27*, 100801. [CrossRef]
38. City of Tshwane. Human Settlements. 2020. Available online: https://www.dffe.gov.za/sites/default/files/reports/environmentoutlook_chapter5.pdf (accessed on 11 August 2023).
39. Statistics South Africa. Census 2011 Metadata. Available online: http://www.statssa.gov.za/census/census_2011/census_products/Census_2011_Metadata.pdf (accessed on 11 August 2023).
40. De Pinho, C.M.D.; Fonseca, L.M.G.; Korting, T.S.; de Almeida, C.M.; Kux, H.J.H. Land-cover classification of an intra-urban environment using high-resolution images and object-based image analysis. *Int. J. Remote Sens.* **2012**, *33*, 5973–5995. [CrossRef]
41. Definiens. Definiens Definiens Developer 7 Developer 7 Reference Book Reference Book. 2007. Available online: www.definiens.comwww.definiens.com (accessed on 11 August 2023).
42. Baatz, M. Multi resolution segmentation: An optimum approach for high quality multi scale image segmentation. In *Beutrage zum AGIT-Symposium*; Salzburg: Heidelberg, Germany, 2000; pp. 12–23.
43. Mugiraneza, T.; Nascetti, A.; Ban, Y. WorldView-2 data for hierarchical object-based urban land cover classification in Kigali: Integrating rule-based approach with urban density and greenness indices. *Remote Sens.* **2019**, *11*, 2128. [CrossRef]
44. Ma, L.; Li, M.; Ma, X.; Cheng, L.; Du, P.; Liu, Y. A review of supervised object-based land-cover image classification. *ISPRS J. Photogramm. Remote Sens.* **2017**, *130*, 277–293. Available online: https://www.sciencedirect.com/science/article/pii/S092427161630661X (accessed on 11 August 2023). [CrossRef]
45. Haralick, R.M.; Shanmugam, K.; Dinstein, I.H. Textural features for image classification. In *IEEE Transactions on Systems, Man, and Cybernetics*; IEEE: New York, NY, USA, 1973; pp. 610–621.
46. Van de Voorde, T.; De Genst, W.; Canters, F.; Stephenne, N.; Wolff, E.; Binard, M. *Extraction of Land Use/Land Cover-Related Information from Very High Resolution Data in Urban and Suburban Areas*; Millpress: Rotterdam, The Netherlands, 2004; pp. 237–244. Available online: https://www.researchgate.net/publication/237134807 (accessed on 11 August 2023).
47. Huete, A.R. A soil-adjusted vegetation index (SAVI). *Remote Sens. Environ.* **1988**, *25*, 295–309. Available online: https://www.sciencedirect.com/science/article/pii/003442578890106X (accessed on 11 August 2023). [CrossRef]
48. Pesaresi, M.; Gerhardinger, A.; Kayitakire, F. A Robust Built-Up Area Presence Index by Anisotropic Rotation-Invariant Textural Measure. *IEEE J. Sel. Top. Appl. Earth Obs. Remote Sens.* **2008**, *1*, 180–192. [CrossRef]

49. White, K.; Walden, J.; Drake, N.; Eckardt, F.; Settlell, J. Mapping the iron oxide content of dune sands, Namib Sand Sea, Namibia, using landsat thematic mapper data. *Remote Sens. Environ.* **1997**, *62*, 30–39. Available online: https://www.sciencedirect.com/science/article/pii/S0034425797000680 (accessed on 11 August 2023). [CrossRef]
50. Stefanov, W.L.; Ramsey, M.S.; Christensen, P.R. Monitoring urban land cover change: An expert system approach to land cover classification of semiarid to arid urban centers. *Remote Sens. Environ.* **2001**, *77*, 173–185. Available online: https://www.sciencedirect.com/science/article/pii/S0034425701002048 (accessed on 11 August 2023). [CrossRef]
51. Chen, X.; Sun, G.; Wang, Z. A case study on the urban impervious surface distribution based on a BCI index. In Proceedings of the International Symposium on Multispectral Image Processing and Pattern Recognition, Enshi, China, 31 October–1 November 2015; Available online: https://api.semanticscholar.org/CorpusID:130192599 (accessed on 11 August 2023).
52. Ukhnaa, M.; Huo, X.; Gaudel, G. Modification of urban built-up area extraction method based on the thematic index-derived bands. *IOP Conf. Ser Earth Environ Sci.* **2019**, *227*, 62009. [CrossRef]
53. Peng, X.; Wu, W.; Zheng, Y.; Sun, J.; Hu, T.; Wang, P. Correlation analysis of land surface temperature and topographic elements in Hangzhou, China. *Sci. Rep.* **2020**, *10*, 10451. [CrossRef] [PubMed]